Polymer-Cushioned Bilayers. II. An Investigation of Interaction Forces and Fusion Using the Surface Forces Apparatus

Joyce Y. Wong, Chad K. Park, Markus Seitz, and Jacob Israelachvili
Department of Chemical Engineering, University of California, Santa Barbara, California 93106 USA

ABSTRACT We have created phospholipid bilayers supported on soft polymer "cushions" which act as deformable substrates (see accompanying paper, Wong, J. Y., J. Majewski, M. Seitz, C. K. Park, J. N. Israelachvili, and G. S. Smith. 1999. *Biophys. J.* 77:1445-1457). In contrast to "solid-supported" membranes, such "soft-supported" membranes can exhibit more natural (higher) fluidity. Our bilayer system was constructed by adsorption of small unilamellar dimyristoylphosphatidylcholine (DMPC) vesicles onto polyethylenimine (PEI)-supported Langmuir-Blodgett lipid monolayers on mica. We used the surface forces apparatus (SFA) to investigate the long-range forces, adhesion, and fusion of two DMPC bilayers both above and below their main transition temperature ($T_m \approx 24°C$). Above T_m, hemi-fusion activation pressures of apposing bilayers were considerably smaller than for solid-supported bilayers, e.g., directly supported on mica. After separation, the bilayers naturally re-formed after short healing times. Also, for the first time, complete fusion of two fluid (liquid crystalline) phospholipid bilayers was observed in the SFA. Below T_m (gel state), very high pressures were needed for hemi-fusion and the healing process became very slow. The presence of the polymer cushion significantly alters the interaction potential, e.g., long-range forces as well as fusion pressures, when compared to solid-supported systems. These fluid model membranes should allow the future study of integral membrane proteins under more physiological conditions.

INTRODUCTION

Lipid vesicles and planar bilayers have been used extensively to model living cells in the biophysical study of molecular mechanisms and fundamental interaction forces involved in phenomena such as the adhesion and fusion of biomembranes (Chernomordik et al., 1987; Sowers, 1987). To fully exploit powerful surface sensitive techniques for this purpose, lipid bilayers have generally been supported on solid substrates (Brian and McConnell, 1984; Tamm and McConnell, 1985; McConnell et al., 1986) and several methods have been developed that allow the measurement of interaction profiles between such membranes with a resolution at the angstrom level (Israelachvili, 1989). The complete force-distance profile can be directly measured with the surface forces apparatus (SFA) (Israelachvili and Adams, 1978; Israelachvili, 1987). This technique has been used to identify and quantify van der Waals, electrostatic, repulsive hydration, and steric forces, and attractive hydrophobic interactions between surfaces in aqueous and nonaqueous solvents (Israelachvili and Adams, 1978; Horn, 1984; Marra and Israelachvili, 1985; Helm et al., 1989, 1992; Israelachvili, 1991; Leckband et al., 1993). In recent years, the SFA was also used for the investigation of more complex biological assemblies, such as the ligand-receptor system biotin-streptavidin (Helm et al., 1991; Leckband et al., 1992, 1994; Wong et al., 1997).

To date, almost all SFA measurements on lipid bilayer membranes have been conducted on a solid mica substrate, which provides an atomically flat surface so that the outer (distal) layer of the substrate-supported membrane can exist in an almost laterally unperturbed fluid state, allowing the adhesion and fusion of model membranes to be followed directly with these systems (Horn, 1984; Marra and Israelachvili, 1985; Helm et al., 1989). However, the direct contact between the inner (proximal) lipid monolayer with the solid substrate surface poses a serious constraint in many systems: various types of membrane deformations and undulations are suppressed and the incorporation of membrane-spanning (transmembrane) proteins with large extracellular and cytoplasmic domains is impossible or highly nonphysiological (Kalb and Tamm, 1992).

The realization of substrate supports that retain the supported membrane's natural hydrophilic environments, fluidity, and freedom to deform would allow the investigation of both equilibrium and dynamic processes such as *gross* membrane deformations and the *molecular* rearrangements of the lipids and membrane-incorporated proteins within and across the bilayers. One promising approach is the use of water-swellable polymers for creating deformable and mobile substrates, resembling the cytoskeleton of living cells (Hvidt and Heller, 1990; Heysel et al., 1995; Jacobson et al., 1995; Janmey, 1995). Recently, such "soft-supported membranes" have been used for the investigation of biomembrane structure and function (Sackmann, 1996), but not the interactions of two membranes. In addition, technical and medical interest arises from their potential use in biosensor systems (McConnell et al., 1986; Stelzle et al., 1993; Sackmann, 1996; Cornell et al., 1997).

Received for publication 6 August 1998 and in final form 25 May 1999.

Address reprint requests to Dr. Jacob N. Israelachvili, Department of Chemical Engineering, University of California, Santa Barbara, CA 93106. Tel.: 805-893-8407/3412; Fax: 805-893-7870; E-mail: jacob@engineering.ucsb.edu.

Joyce Y. Wong's current address is Department of Biomedical Engineering, Boston University, Boston, MA 02215.

0006-3495/99/09/1458/11 $2.00

In the work presented here we have constructed phospholipid dimyristoylphosphatidylcholine (DMPC) bilayers on a soft polymer cushion for SFA and related measurements (Fig. 1; see also accompanying paper, Wong, J. Y., J. Majewski, M. Seitz, C. K. Park, J. N. Israelachvili, and G. S. Smith. 1999. *Biophys. J.* 77:1445-1457, hereafter referred to as part I). The use of branched polyethyleneimine (PEI), which is positively charged in aqueous solutions below pH 9, allows the electrostatic fixation of the polyelectrolyte substrate onto the negatively charged mica or silica surfaces used in such experiments. Furthermore, branched PEI swells in water so that an aqueous compartment can build up between the membrane and the mica substrate (Chen and Israelachvili, 1992; part I).

In this paper we report our first SFA measurements of physisorbed zwitterionic DMPC bilayers on PEI-covered mica substrates, with a focus on the comparison with previously investigated phospholipid bilayers that were directly supported on mica. Independent structural studies were performed in part I of our studies, which confirmed the structure of the polymer-cushioned bilayer. Also, the convenient phase transition temperature between the gel and liquid crystalline phases of DMPC bilayers of $T_m = 24°C$ (Janiak et al., 1976) allowed us to study the effect of membrane fluidity on the intermembrane forces and fusion mechanisms.

EXPERIMENTAL PROCEDURES

Construction of supported bilayers

Various preparation techniques have been suggested for mono and multilayer systems, such as the Langmuir-Blodgett (LB) technique (Tamm and McConnell, 1985) and self-assembly processes on planar surfaces (Brian and McConnell, 1984; Kalb et al., 1992; Lang et al., 1992), or on small glass beads (Bayerl and Bloom, 1990). We chose a stepwise preparation of the supported bilayer in which the first or inner ("proximal") DMPC monolayer was transferred onto the mica substrate from a polyelectrolyte-containing subphase by the LB method. The second layer was created by spreading unilamellar vesicles onto these preformed polymer-supported monolayers, as reported in the literature for the formation of other bilayer systems supported on solid substrates (Kalb et al., 1992; Lang et al., 1992; Spinke et al., 1992; Kühner et al., 1994). Several other procedures were also tried, but the one described here proved to be the most reliable and versatile (for more details, see part I, Fig. 7 *b*). Besides, this approach provides two advantages: first, the sample preparation can easily be done within the SFA (or another type of measuring cell) on preinstalled surfaces. Second, this method should allow the incorporation of membrane proteins directly from proteoliposomes.

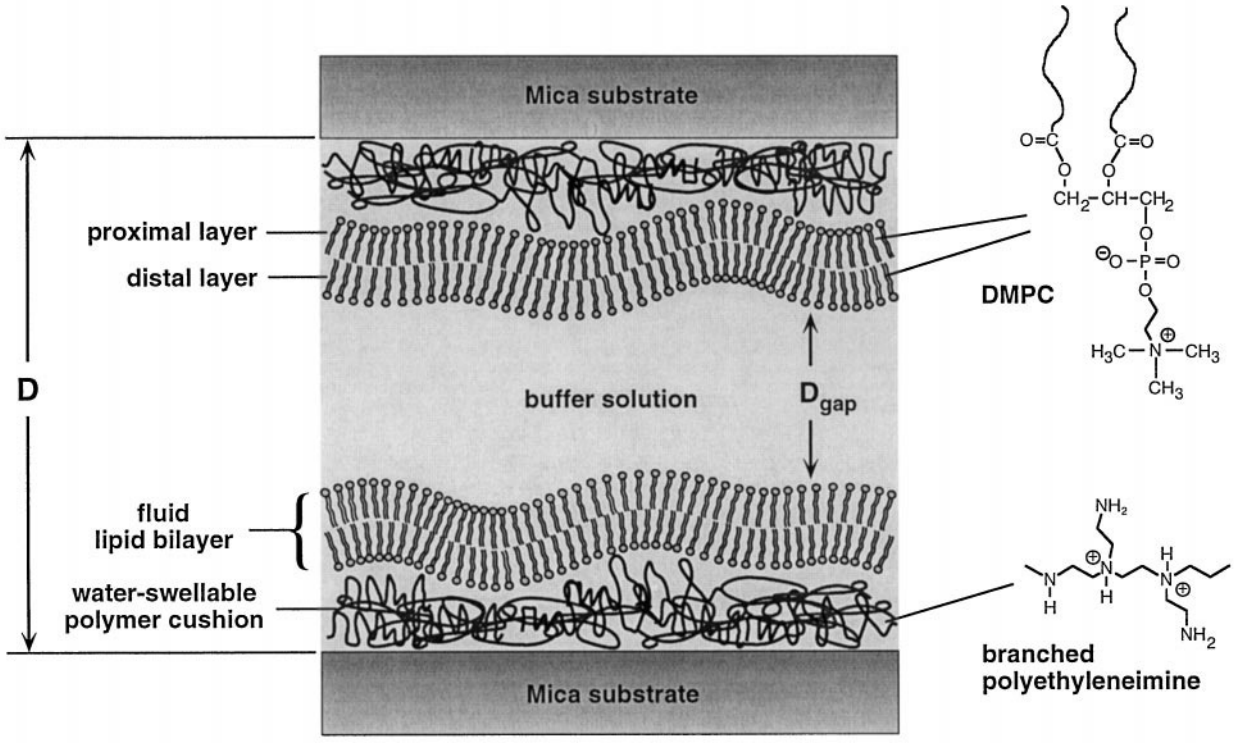

FIGURE 1 Polymer-supported bilayer membranes for SFA measurements. The zero position ($D = 0$) is defined for the two mica substrates in contact. The mean bilayer-bilayer separation D_{gap} is at least 8 nm less than D.

Materials

DMPC (purity >99%) was purchased from Avanti Polar Lipids (Alabaster, AL) and used without further purification. Potassium nitrate (purity 99.994%) was from Alfa (Ward Hill, MA). Branched PEI (M_n = 1800 g/mol) was obtained from Polysciences (Warrington, PA). To roughly estimate the Flory radius of this polyelectrolyte in water (good solvent) from $R_F = l_o \times (M_n/M_o)^{3/5}$ (Israelachvili, 1991), we assume a linear polymer structure. With a repeat unit length of $l_o \approx 0.38$ nm, and a monomer molecular weight of M_o = 43 g/mol, we obtain $R_F \approx 3.6$ nm.

All other solvents and materials were purchased from Fisher (Pittsburgh, PA). Water was double-distilled and purified through a Milli-Q filter system (Millipore Corp., Bedford, MA).

Preparation of DMPC vesicles

Small unilamellar vesicles (SUVs) of DMPC were freshly prepared before each measurement by a procedure described in the literature (Bangham et al., 1974). Briefly, multilamellar vesicles (MLVs) were prepared by hydrating a dried lipid film of DMPC with Millipore water (37°C), subsequently sonicated with a probe sonicator (Fisher Sonic Dismembrator 300), and filtered through a 0.22-μm Millipore filter. The resulting SUVs have an average diameter of 40 nm as found by particle sizing measurements (Microtrac UPA 150, Brookhaven Instruments Corp.), and were stored at 28°C (above the gel-fluid phase transition) before use to prevent their aggregation.

Preparation of DMPC bilayers on PEI/mica

Polymer-supported monolayers were prepared by LB-deposition using a temperature-controlled Wilhelmy trough (Joyce-Loebl Co., Malden, MA). All of the following preparations were carried out in a laminar flow box (Labconco, Kansas City, MO). Freshly prepared back-silvered mica substrates glued onto silica disks were lowered into an aqueous subphase containing 100 ppm PEI and 0.5 mM potassium nitrate. A monolayer of DMPC was then spread from chloroform solution ($\sim 10^{-3}$ mol/l) onto the polymer-containing subphase. It was noted that the isotherms of DMPC were indistinguishable from published curves measured on a pure-water subphase. The monolayer was compressed to 30 mN/m (mean molecular area = 0.6 nm^2) at 20°C, with compression rates between 0.03 and 0.05 nm^2/(molecule-min). After an expansion and recompression, the DMPC monolayers were equilibrated for at least 30 min, and finally transferred onto the mica substrates. The dipping speed during transfer was 5 mm/min; reproducible transfer ratios (between 0.95 and 1.1) were observed. After the installation of the samples into the SFA, the apparatus was kept in a temperature-controlled room set to 28°C (above the gel-fluid phase transition temperature of DMPC bilayers, T_m = 24°C) and filled with a 0.5-mM potassium nitrate solution containing small unilamellar DMPC vesicles ($\sim$0.3 mg/ml).

Surface forces apparatus

The SFA used in the surface forces measurements has been described extensively (Israelachvili and Adams, 1976; Israelachvili and McGuiggan, 1990). The distance between the two surfaces during the experiments was visualized using the optical interference technique described previously (Israelachvili, 1973; Helm et al., 1992). Briefly, fringes of equal chromatic order (FECO) are produced when white light is passed through the opposing sample surfaces, and reflect the shape of the surface contact region. Thus, the distance of the two mica surfaces and the topography of the contact region can be followed at the same time. In the force-distance curves shown in this paper, $D = 0$ corresponds to the contact of the bare mica substrates (Fig. 1), which was determined before each experiment. Note that, as the disks had to be taken out of the SFA for the monolayer deposition, the *absolute* zero position is only known to an accuracy of $\sim$1 nm. However, this yields an ambiguous thickness only for the underlying *compressed* polymer layer; the relatively measured distances in the force profile are known to greater accuracy, typically 0.2 nm. Also, polymer thicknesses were determined in independent control measurements in the absence of bilayers.

RESULTS

As seen in part I of these studies, the resulting structure from vesicle adsorption onto a polymer-supported monolayer of DMPC is a nearly complete bilayer atop a highly hydrated polymer film (nearly 15 nm thick; see part I, Table 4 and Fig. 7). This is in contrast to other methods that resulted in incomplete coverage or excess coverage of the lipids (see part I, Figs. 3 and 6, Table 3). Additional proof of this structure was obtained by independent fluorescence studies (Seitz et al., 1999).

Forces between adsorbed PEI layers (no bilayers)

Fig. 2 shows the force profile between two mica surfaces coated with branched PEI *without* lipid. An exponentially repulsive double-layer interaction was measured at long range, as expected. At smaller distances ($D < 3$ nm) a steep increase in the force was observed. This is attributed to the steric repulsion of the two adsorbed polymer layers as they are pressed into hard contact. On further increasing the pressure, the two layers could be compressed to $D \approx 2$ nm ($\sim$1 nm per layer). The contribution of free PEI in solution to the interaction profile can be neglected, because the osmotic pressure limit at a concentration of 100 ppm is

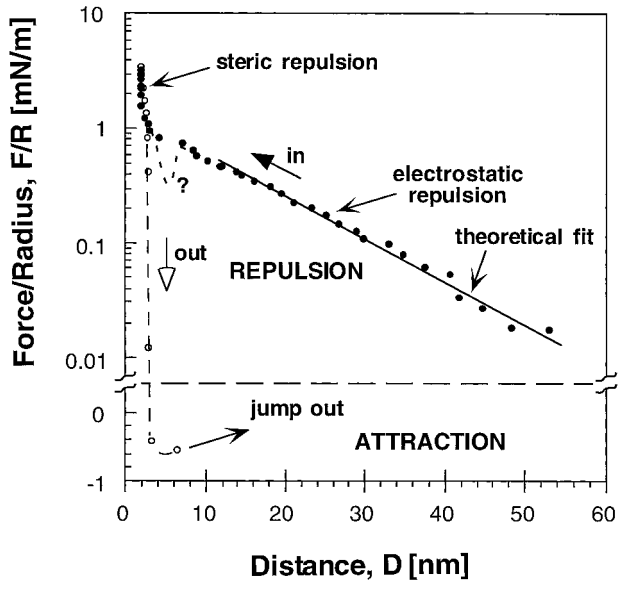

FIGURE 2 Interaction profile of two mica surfaces covered with layers of branched PEI adsorbed from solution (100 ppm in 0.5 mM KNO_3) at 28°C. *Filled symbols,* compression (including a theoretical fit of the long-range force based on electric double layer theory, using a Debye length of $\kappa^{-1}_{(exptl.)} = 11.7$ nm and assuming that the plane of effective charge (Helmholtz plane) coincides with the mica surface ($D = 0$), for which we obtain a surface potential of $\psi_o = 50$ mV). *Open symbols,* expansion data.

much less than the measured values. Finally, it should be mentioned in this context that for adsorbed layers of linear polycations, such as polystyrene sulfonate of polyallylamine, on mica, a thickness of typically 0.8 nm has been reported in the literature (Decher and Schmitt, 1992; Lowack and Helm, 1995).

On subsequent expansion of the two compressed PEI layers, adhesion "jumps" out of contact were measured from which an adhesion energy of $W = -F/2\pi R = 0.10 \pm 0.05$ mJ/m^2 could be calculated. This adhesion is most likely to be due to molecular entanglements and polymer "bridging" forces. As expected for such polymer surfaces, this adhesion energy increased with the time that the surfaces were kept in contact, and with the applied pressure. Note that the compression curve contains a "plateau" in the force curve between 7 and 4 nm, which may indicate adhesiveness already on approach.

Forces and fusion of DMPC bilayers physisorbed onto PEI

A typical force-distance curve between two DMPC bilayers physisorbed on branched PEI/mica prepared as described above ($T = 28$°C, 0.5 mM KNO_3) is shown in Fig. 3. The interaction profile during compression of the system (Fig. 3, *solid arrows*) exhibits four characteristic regimes.

Long-range force regime: a long-range exponential repulsion starting at $\sim D \approx 50$ nm, which is also shown on a logarithmic plot in the inset (IN curve).

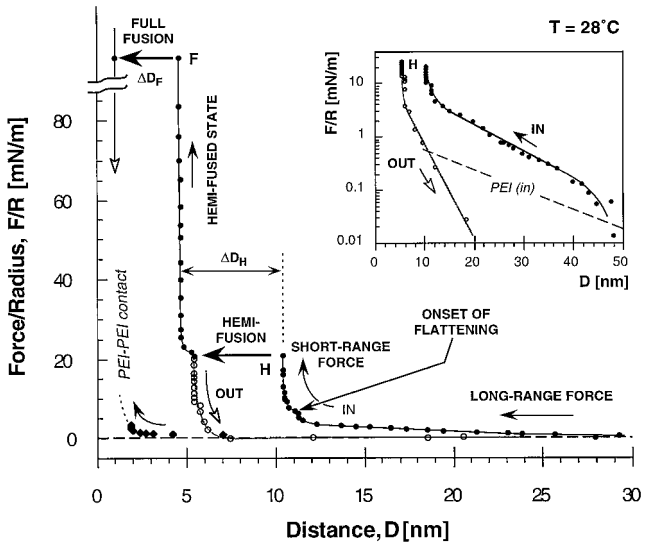

FIGURE 3 Interaction force profile of two physisorbed DMPC membranes on PEI, prepared by vesicle fusion onto polymer-supported monolayers at 28°C in 0.5 mM KNO_3 solution. *Filled symbols,* compression; *open symbols,* expansion or separation after hemi-fusion; *dotted line*, extrapolation of the PEI-PEI interaction profile (*diamond symbols*). *Inset:* logarithmic plot of the long-range interaction forces on compression and expansion after hemi-fusion at *H*. *Dashed line in inset:* compression force between two PEI layers without adsorbed bilayers (same as Fig. 2), for comparison.

Short-range force regime: a steep increase in the repulsion at $D \approx 10$–11 nm, just before the bilayers hemi-fuse. We note that at $D \approx 10$ nm the distance between the bilayers, D_w, is much less, closer to $\sim$1 nm, as shown in Fig. 1.

Hemi-fused state: at small distances (points *H* in Fig. 3), a discontinuity occurs at $F/R \sim 20$ mN/m, characterized by a sudden and spontaneous decrease of the distance between the two mica surfaces from $D = 10.5$ to 5.5 nm. This is the hemi-fusion transition. The hemi-fused state persists up to a pressure of 50–100 atm, and a separation of $D = 4.5$ nm.

Full fusion: at very high F/R values, corresponding to a compressive pressure between the now-flattened bilayers of 50–100 atm, another discontinuity occurs at point *F* when the hemi-fused bilayer ruptures and the mica surfaces move in from $D \approx 4.5$ nm to $D \approx 1$ nm.

At the point of hemi-fusion (*H*), the change in the interference (FECO) fringe pattern is consistent with the complete removal of one bilayer from the interaction zone such that only one bilayer membrane remains in the contact region. During this hemi-fusion process either the center or the outer edge of the curved contact region "broke through" (cf. Fig. 6 below). The corresponding distance between the two mica surfaces at these spots or "fusion sites" decreased by $\Delta D_H \approx 5$ nm. These spots then slowly spread out toward the side or toward the center of the contact region until, eventually, the whole interference pattern was shifted by the same amount to smaller wavelengths (smaller distances). This process usually took $\sim$2–5 s. These observations have been described already for fully developed bilayers that were directly deposited onto mica by Horn (1984) and Helm et al. (1989, 1992). However, these solid-supported bilayers underwent hemi-fusion at much higher compressive pressures.

In general, the forces recorded during expansion of the system followed the previous compression curves, i.e., the long-range forces were (almost) reversible, so long as the surfaces were not brought in close enough for hemi-fusion to occur (i.e., for $D > D_H$). However, slightly smaller forces were measured on expansion as compared to the initial compression of the bilayers (data not shown). This hysteresis was more pronounced after higher pressures were applied to the system in contact (but not hemi-fused). Once the two bilayers had been hemi-fused, the force on separation was completely different, falling significantly faster on separation than on the original compression (cf. OUT curve in Fig. 3). However, no large adhesion was found, although in some cases a slight "jump" out of contact was observed after a separation from the hemi-fused state. In those cases, an adhesive force of $F/R \approx -0.02$ mN/m was typically obtained. After a separation from the hemi-fused state, if the surfaces were kept well-separated for several hours, both bilayers healed and gave rise to the same force profiles as a previously unfused sample. However, for insufficient healing times, the force on recompression was decreased.

Full fusion of the PEI-supported membranes could be induced at high pressures ($P > 50$ atm) resulting in a final discontinuous decrease of the mica-mica separation distance

by $\Delta D_F = 3.5$ nm (Fig. 3, point *F*). During full fusion the remaining DMPC bilayer was completely removed from the gaps and, after separation, it did not recover within the time of the experiments (16 h after fusion and separation).

Effect of temperature on the forces and fusion of polymer-supported DMPC bilayers

Fig. 4 shows the temperature dependence of the short-range repulsive interaction as measured in the gel state at 21°C and in the liquid-crystalline (fluid) state at 28°C (i.e., below and above $T_m = 24$°C, respectively). At the lower temperature, the "hard wall" is shifted out to larger distances by 1.4 nm. In addition, the fusion barrier, i.e., the pressure required to achieve hemi-fusion of the two apposing membranes, drastically *increases* in the gel state. At 21°C, no hemi-fusion was observed up to compressive pressures of $P = 30$ atm ($F/R \sim 70$ mN/m as shown in Fig. 4), and could only be achieved at pressures where *fluid* membranes undergo *full* fusion ($P > 50$ atm).

"Healing" of bilayers after fusion

Once hemi-fusion was achieved in the gel state at 21°C, the physisorbed DMPC bilayer no longer healed to reform a full bilayer within the time scale of our experiments (~16 h). This is in contrast to the findings at 28°C, where the bilayers healed completely within a few hours. The healing of the PEI-supported DMPC bilayers after hemi-fusion and separation is illustrated in Fig. 5 by three successive measurements taken at the same contact spot. *Curve A* shows the interaction profile at 21°C, which was already discussed above, followed by a forced hemi-fusion at high pressures ($P > 50$ atm). *Curve B* was measured at 21°C 6 h *after* the hemi-fusion. Only an exponential repulsive force was detected until a hard wall at 5 nm was reached, which corresponds to one DMPC bilayer and two compressed PEI layers in the gap between the two mica surfaces. Complete recovery of the second bilayer was achieved only after heating the system above the phase transition temperature to the fluid state. This is shown by *curve C*, which was measured 14 h after *curve B*, and which is very similar to the force between freshly prepared DMPC bilayers in the fluid state at 28°C (cf. Fig. 3).

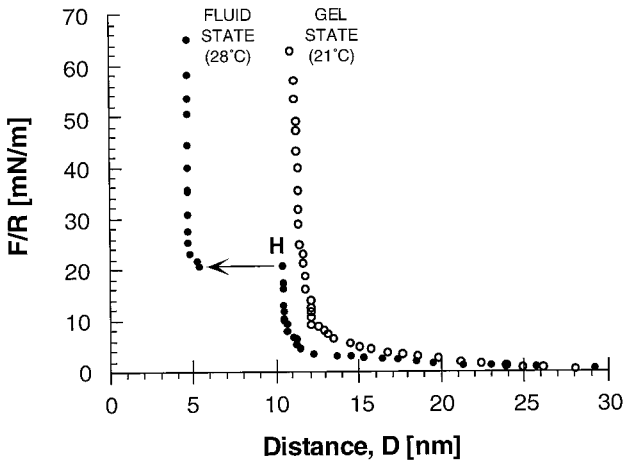

FIGURE 4 Temperature dependence of the interaction profile between two DMPC membranes in 0.5 mM KNO_3. *Closed symbols,* measurement at 28°C, hemi-fusion indicated by an arrow (same data as in Fig. 3). *Open symbols*, measurement at 21°C.

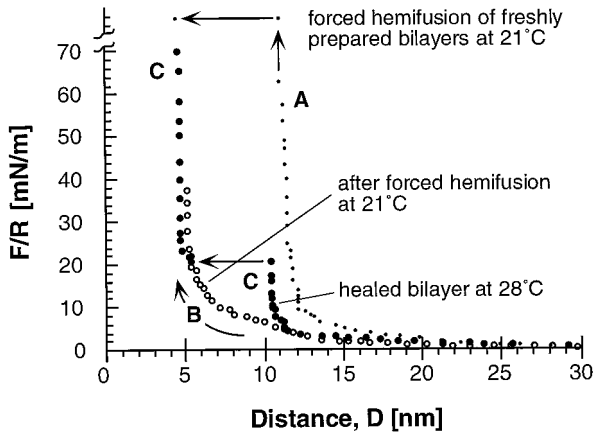

FIGURE 5 Healing of a lipid membrane after hemi-fusion. (*A*) freshly prepared gel-state bilayers, forced to hemi-fuse at 21°C. (*B*) Force measured 6 h after forced hemi-fusion, at 21°C. (*C*) Force measured 14 h after forced hemi-fusion at 21°C, followed by separation then heating to 28°C.

DISCUSSION

As discussed in part I, there is a balance of the interaction forces between the various components of the polymer-supported lipid bilayer system. There is a strong interaction between the PEI layer and the substrate, because it was shown in part I and a previous study (Majewski et al., 1998) that PEI added to a pre-formed substrate-supported bilayer could form a layer *underneath* the bilayer. Furthermore, there is an interaction between the lipid bilayer and the polymer layer, as the bilayer cannot be removed after extensive washing (see part I, Method 3). However, this interaction is not as strong as the interaction between PEI and the mica substrate because the lipid layers remain fluid and are able to undergo complete fusion in the SFA. Moreover, fluorescence studies (Seitz et al., 1999) revealed that a bleached spot is able to recover, which is in agreement with the observed fluidity in the SFA (i.e., healing after hemi-fusion). We note, however, that the PEI layer may also penetrate somewhat into the bilayer.

Measured bilayer dimensions at different temperatures

The temperature dependence of the bilayer dimensions, which can be extracted from the force profiles between PEI-supported DMPC bilayers, is summarized in Table 1,

TABLE 1 Comparison of temperature-dependent bilayer dimensions (in nm) as determined by SFA measurements and by x-ray diffraction

	Total Thickness (D)		Hydrated Bilayer Thickness ($D_B + D_w$)		Unhydrated Bilayer Thickness (D_B)	
Phase State and Temperature*	SFA $2D_B+D_w+2D_{PEI}$	X-ray# $2D_B+D_w$	SFA ΔD_H	X-ray#	SFA ΔD_F	X-ray#
Gel State $T_1 < T_m$	11.8	10.94	6.5	6.5	—	4.45
Fluid state $T_2 > T_m$	10.4	9.56	5.7	6.0	3.5	3.55
Thickness Difference $D(T_1) - D(T_2)$	1.4	1.38	0.8	0.5	—	0.9

For definitions of distances and thicknesses see Fig. 6.
*For SFA measurements, $T_1 = 21°C$, $T_2 = 28°C$; for X-ray diffraction, $T_1 = 20°C$, $T_2 = 37°C$ (Janiak et al., 1976).
#Thicknesses determined from x-ray diffraction on multilamellar systems (Janiak et al., 1976).

and the various dimensions of the system are defined in Fig. 6. When the two membranes have come into close, "hard" contact, there is still a "hydration" layer of water, D_w, separating the lipid headgroups. We note that the thickness difference on cooling from the fluid to the gel state of our hydrated bilayers correlates well with the expected increase from literature-reported x-ray diffraction studies. Thus, in excess water, a value of $D_B = 3.55$ nm for a DMPC bilayer in the L_α phase (at 37°C) was determined, whereas in the $P_{\beta'}$-phase (at 20°C) an increase to 4.45 nm was found (Janiak et al., 1976). Considering the slightly lower thickness of the reported hydration water layer, D_w, in the gel phase (2.04 nm at 20°C compared to 2.45 nm at 37°C), a total shift of the hard wall, $D = 2D_B + D_w + 2D_{PEI}$, by 1.38 nm can be calculated (Table 1). Our SFA results (1.4 nm) are in excellent agreement with this value. Note that this assumes no thickness change of the underlying polymer layer, D_{PEI}, in this temperature range. From the above, the thickness of the underlying polymer layer under compression can be calculated to be $D_{PEI} \sim 0.5$ nm per layer. Although the experimental error of this value is also 0.5 nm per layer due to the ambiguity of the absolute zero position (cf. Experimental section), it is still in good agreement with the thickness determined in our measurements on the pure PEI layers (Fig. 2).

Additional evidence for a thickening of DMPC bilayers at lower temperatures ($T < T_m$) is given by the increase in the value for ΔD_H (Table 1): the abrupt change in thickness found when hemi-fusion is initiated between the two biomembranes. Again, these values are in good agreement with values predicted from x-ray diffraction (Janiak et al., 1976) when considering that the hemi-fusion process results in a complete removal of one hydrated bilayer ($\Delta D_H = D_B + D_w$). As described earlier, full fusion was observed only when the DMPC bilayer was in the fluid state, and the value for ΔD_F is the same as the value of D_B found from x-ray studies (Table 1). In addition, the position of the hard wall after full fusion coincides with the hard wall position of two PEI layers in contact (Fig. 3), indicating the final complete removal of *both* bilayers.

Fusion pathways

Two possible hemi-fusion pathways that would satisfy the observed changes in our system are shown schematically in Fig. 6. In case *A*, one membrane "ruptures" at a defect which then spreads out laterally (Fig. 6 *A*). The other possible mechanism involves the hemi-fusion of the two outer membrane monolayers (Fig. 6 *B*). Although the first process cannot be entirely excluded, especially above T_m where the fluid bilayer may spread out more easily on the soft support, the latter mechanism is generally favored in the literature as an intermediate step during the fusion of bilayer vesicles (Chernomordik et al., 1987) or for the hemi-fusion of solid-supported lipid bilayers (Horn, 1984; Helm et al., 1989, 1992). One can distinguish between these two scenarios by comparing the pressures required for hemi-fusion and full fusion. Referring again to Fig. 6, in the case of *A-A′* one would expect two similar breakthrough mechanisms for both rupture steps of presumably similar activation barriers. Case *B-B′* suggests that two different mechanisms, and presumably pressures, are required for the two different fusion steps at *B* and *B′*, which is what we observe (as discussed below, the observed pressures differed by an order of magnitude).

Fusion pressures and activation energies (or energy barriers) for polymer-supported and solid-supported bilayers

The pressure required for the hemi-fusion of two polymer-supported DMPC bilayers can be calculated using two different approaches. In the first method, the pressure between two planar lipid bilayers, P_{planar}, can be obtained by applying the Derjaguin approximation (Israelachvili, 1991) to the measured forces, then differentiating the resulting energy. This gives $E_{planar} = F_{curved}/2\pi R$ and $P_{planar} = -dE_{planar}/dD$, where F_{curved} is the force measured between the polymer-supported bilayers on the curved mica surfaces, R is the undeformed radius of curvature, and D is the measured distance between the two surfaces. The values required for hemi-fusion of DMPC bilayers in the fluid state (at 28°C)

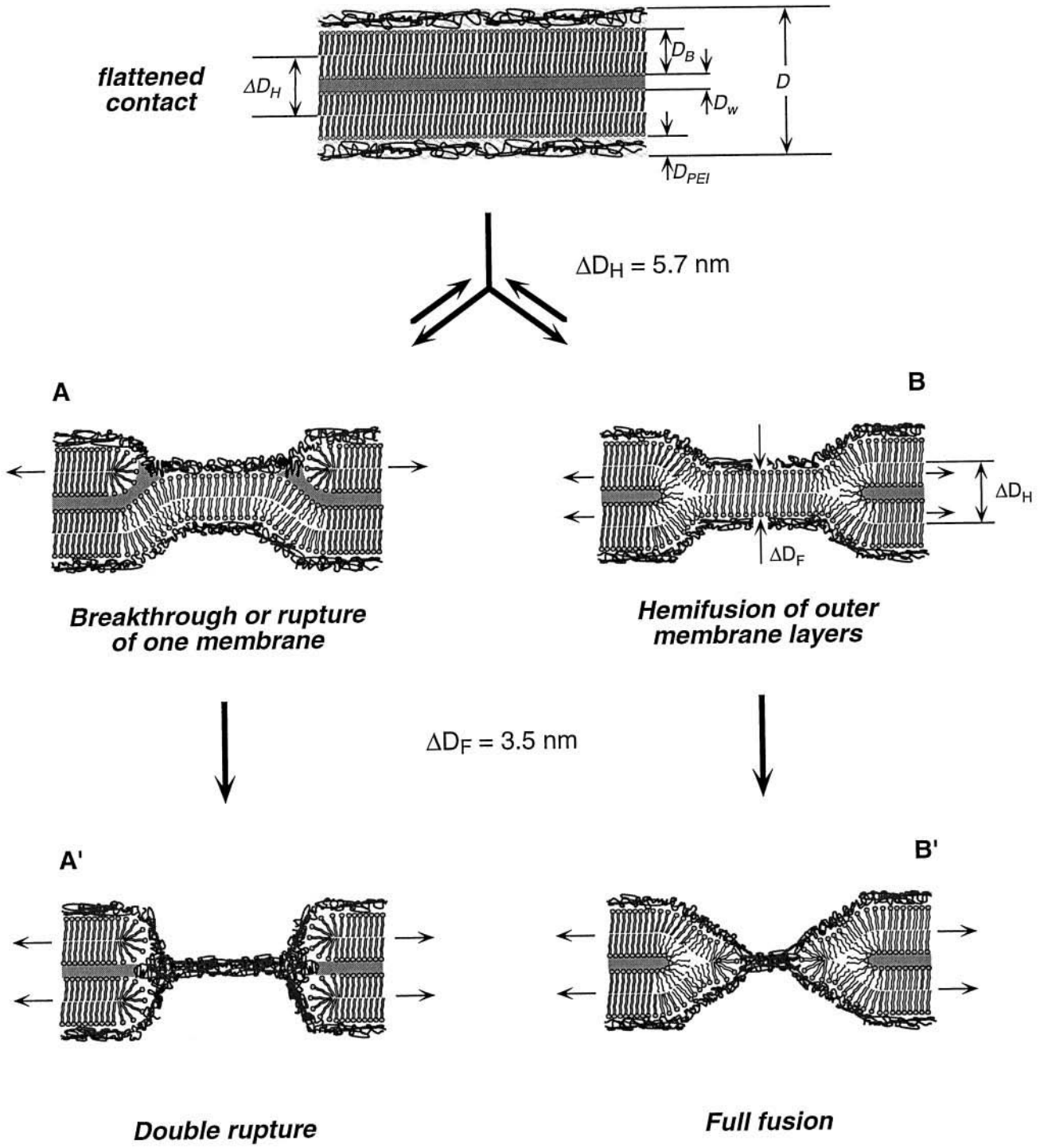

FIGURE 6 Schematic representation of possible hemi-fusion pathways for PEI-supported DMPC bilayers. *Right:* schematic of what is "seen" on the FECO fringe pattern and how two vesicles would deform during hemi-fusion (*H*) and full-fusion (*F*).

obtained from this method lie within the range $P_{\text{planar}} = (0.3–2.0) \times 10^7$ N/m^2 $\approx$ 30–200 atm. However, at these relatively high pressures the surfaces flatten considerably in the contact region and the Derjaguin approximation can no longer be used, so that pressures calculated from the force profile by differentiation in this regime are generally too high.

An alternative way of estimating the fusion pressure is to simply divide the (measured) force at which hemi-fusion occurs by the (also measured) area of flattened contact. From the results at 28°C shown in Fig. 3, $P_{\text{planar}} \approx 10$ atm was obtained ($F/R = 21.5$ mN/m, $R = 1.5$ cm, $F = 0.32$ mN, contact area $A \approx 400$ μm^2). The values of the hemi-fusion pressure obtained by the latter method varied slightly

between different measurements, but typically fell between 7 and 10 atm, corresponding to measured forces of $F/R \approx 20$–25 mN/m. These variations may in part be explained by time and rate effects due to different compression rates and contact times. Also, the time span between two successive experiments on the same contact spot affects the hemi-fusion barrier. As expected, lower values were generally measured on recently hemi-fused membranes and on membranes that were left close to contact for long periods of time.

It is interesting to compare these results with earlier results on the fusion of solid-supported bilayers (Horn, 1984; Helm et al., 1989, 1992). In contrast to our measurements on polymer-supported bilayers, previous investigations showed that two fluid DMPC distal layers in bilayers that were directly supported on solid DPPE-coated mica cannot be hemi-fused up to pressures of ~40 atm when calculated using the second (preferable) method above (Helm et al., 1989). Moreover, hemi-fusion could only be realized in solid-supported systems with packing defects, e.g., bilayers with specific weak points such as grain boundaries, bilayers with dissolved solvents, or heterogeneous bilayers such as "egg PC" (Horn, 1984). Even in these cases, pressures of up to $P = 50$–100 atm were needed to achieve hemi-fusion (Horn, 1984; Helm et al., 1992). Finally, full fusion as found for the PEI-supported bilayers described here was not previously observed with the SFA between bilayers deposited directly onto mica, where full removal of both lipid layers would have resulted in direct mica-mica contact (Horn, 1984; Helm et al., 1989, 1992).

Bilayers directly supported on solid substrates such as mica are restricted in the mobility of their inner lipid monolayer due to the proximity of the solid substrate. Furthermore, these systems were often composed of a proximal, solid-like DPPE layer on which the second, fluid lipid layer was transferred from the air-water interface. When cooled to the gel state, the mean molecular area per lipid decreases, which results in packing stresses and hole formation in the distal DMPC layers, since the supporting DPPE layers cannot accommodate these changes. In contrast, DMPC bilayers on polymer supports can stay intact while undergoing the phase change from the fluid L_α to the $P_{\beta'}$ gel phase as a whole, reducing the number of defect sites, and increasing the fusion pressure. Furthermore, when comparing the two different bilayer systems, we have to consider not only the influence of the soft polymer support but also the presence of DMPC vesicles in our experiments (this will be important later in the discussion). Above the phase transition temperature of DMPC bilayers from the gel- to the fluid-state, both factors may promote the healing process, resulting in nearly complete recovery of the DMPC bilayers after hemi-fusion. This suggests the free mobility of lipids within the polymer-supported membranes in our experiments at 28°C.

Similar to the calculation of the fusion pressure, the *energy* barrier for the hemi-fusion event normalized by the radius of curvature of the bilayers, E_{curved}/R, can be calculated by integrating the measured force curve from infinity to the respective distance at which fusion occurred. Again, in the region in which the surfaces flatten considerably, this value can be better estimated by multiplying the measured F/R at hemi-fusion by the normal distance between the bilayers over which flattening occurs. From E_{curved}/R, the "fusion energy" of *one* DMPC vesicle, E^{fus}, in the liquid-crystalline phase can be deduced as

$$E^{fus} = 1/2(E_{curved}/R_{SFA}) \times R_{ves} \quad (1)$$

From the curve shown in Fig. 3 we obtained values of $E_{curved}/R = 5.2 \times 10^{-11}$ J/m by integration, and $E_{curved}/R = 2.1 \times 10^{-11}$ J/m by multiplication of F/R by the ~1 nm normal displacement during flattening (cf. flattening onset in force profile, Fig. 3). We choose the second value for the calculation of E^{fus}, since an integration of the interaction forces between soft-supported bilayers also includes long-range repulsive contributions (such as undulations), which may not exist in small vesicle systems, and also because this approach tends to overestimate the fusion pressure. Thus, for fluid bilayers of DMPC our experiments lead to the following equation for the fusion energy barrier of vesicles or curved bilayers:

$$E^{fus}(\mathrm{J}) = 10^{-20} \times R(\mathrm{nm}), \quad (2)$$

where R is the radius of the vesicle or bilayer taken as a "normalization" factor to convert from nearly planar polymer-supported bilayers ($R \approx 1$ cm) to spherical vesicles of smaller size, and excludes any effects due to curvature stresses (see below). The value calculated from Eq. 2 gives a lower boundary for E^{fus}. Based on the variability in our data for E_{curved}, the upper boundary is estimated to be at most five times that number. For example, for small vesicles having a typical radius of $R \approx 10$ nm, at 300 K, we obtained $E^{fus} \approx 2 \times 10^{-19}$ J. This corresponds to ~25 k_BT per vesicle. Note that in the gel state no fusion was observed even up to twice this value.

Comparison with previous fusion studies

We have observed that the fusogenicity, as evidenced by the measured fusion pressure, is higher for fluid-like bilayers. At first glance, this result seems to contradict findings on free unilamellar vesicles in solution for which fusion of the bilayer membranes was found to be favored *below* the fluid-gel transition, T_m (Chernomordik et al., 1987; Sowers, 1987; Israelachvili, 1991). However, this difference can be understood by considering that compared to nearly planar bilayers, small, highly curved vesicles in the gel state are in a highly stressed (faceted) state, which they can overcome by fusing into larger vesicles. Also, in addition to the aforementioned changes in the internal packing, many fusogenicity studies on free vesicles naturally include a generally enhanced aggregation tendency below T_m. Whereas the first effect introduces an actual driving force for the actual fusion process, the latter simply enlarges the absolute

amount of fusion events by increasing the number of contacting bilayers.

Because the SFA technique allows positioning of two apposing bilayers at any separation, our results exclude this "aggregation effect." As discussed above, earlier SFA investigations on solid supported systems suggest that the immobile inner DPPE layers provide a strong hydrophobic "intermembrane" force when they are exposed to the aqueous environment as a result of defects or stresses in the outer lipid monolayers (Helm et al., 1989, 1992). Their interaction is assumed to drive the hemi-fusion in these systems. Packing defects, lateral phase separation, and lipid shape can all contribute to such defects or stresses, and similar effects can frequently be induced by cooling the layers into the gel phase especially when the bilayers are highly curved, as in small vesicles. In the soft-supported systems investigated here, a further factor facilitating fusion was found to be the bilayers increased fluidity above their melting transition temperature.

This observation agrees well with studies by Ohki et al. (Breisblatt and Ohki, 1975; Ohki, 1993) who reported the temperature effect on the full fusion of *large* unilamellar vesicles in contact (termed spherical bilayer doublets). These phosphatidylcholine membranes, with their large radius of curvature ($R \approx 2$ mm), are more comparable to our nearly planar bilayer systems ($R \approx 1$ cm) than small vesicles. Although the percentage of fusing bilayer doublets at 25°C was very small, there was a sharp increase at temperatures more than 20°C above the melting temperature of the bilayers (the so-called "fusion threshold" temperature, which for DMPC was reported as $T_f = 59°$), before plateauing close to the temperature at which the membranes ultimately rupture. It has been argued that by increasing the fluidity of the membrane, the freedom of motion of the hydrocarbon chains of lipid molecules can be increased so as to allow the hydrocarbon chains to be exposed at the membrane surface (Ohki, 1993).

Our current results taken together with the earlier work clearly show that several factors play a crucial role in the fusion of lipid bilayer membranes. However, it is important to distinguish between such factors promoting bilayer aggregation and those promoting fusion. Although bilayer contact is an essential requirement for each fusion event, many systems may remain in the thermodynamically or kinetically favored aggregated state. This shows that large adhesiveness between biological membranes does not necessarily imply a large fusogenicity. Conversely, as in our case of soft-supported bilayers, the lack of significant adhesion does not prevent the fusion event. Indeed, once forced into close contact, our measured fusion barrier was actually lower than those found for many previously investigated adhesive solid-supported systems. *Our artificial positioning of bilayers may thus resemble the action of fusion-promoting proteins found in nature*, without which the energetics of the system would prevent close contact of highly fusogenic membranes. This is highly relevant, as recent structural studies of membrane fusion proteins have led to a proposed mechanism that implies that an important role of membrane fusion proteins is to cause close membrane apposition needed for membrane fusion (Skehel and Wiley, 1998).

Long-range interactions between polymer-supported membranes

Finally, the weaker interaction forces at larger distances need to be addressed (Fig. 3). At mica-mica separations above 20 nm, the repulsive force falls exponentially with a characteristic decay length of ~10 nm. At first sight, this value agrees fairly well with the expected Debye length κ^{-1} of a repulsive electrostatic interaction in 0.5 mM 1:1-electrolyte solution, for which $\kappa^{-1}_{(\text{theoret.})} = 13$ nm (Israelachvili, 1991). However, compared to the interaction curve of pure PEI layers under the same conditions (Fig. 3, *inset*) for which the long-range forces could be fitted to the Poisson-Boltzmann equation (Debye length, $\kappa^{-1}_{\text{exptl.}} = 11.7$ nm; $\psi_o = 50$ mV), attempts to fit the experimental data of PEI-supported DMPC bilayers for a realistic ψ_o failed. In order to avoid an unrealistically high surface potential ψ_o, a large shift of the plane of effective charge ("Stern layer") along the surface normal had to be assumed; e.g., for constant surface potentials of $\psi_o = 40$ and 100 mV, Stern shifts away from each mica surface of 20 or 8 nm, respectively, are necessary to fit the experimental data. More importantly, at higher potassium nitrate concentration (150 mM, $\kappa^{-1} \sim 0.8$ nm), where the electrostatic interaction should be almost completely suppressed, nearly the same long-range repulsive force was measured (data not shown). Finally, it seems unlikely that such large and long-range forces would be caused by undulation modes of the fluid lipid membrane alone. Also, one would expect these modes to be altered in the gel state of the membrane at 21°C, but this was not the case, as essentially identical long-range behavior was found.

One possible explanation for the additional repulsive interaction would be the presence of vesicles in the region of the bilayer-bilayer contact (physisorbed to the surfaces or present in solution), which are pushed out of the contact region, slowly but reversibly, during the approach of the surfaces. In control experiments, however, the complete preparation was done outside the SFA at high temperature to prevent aggregation of the vesicles (Spinke et al., 1992). This preparation included an extensive rinsing step with salt solution after the surfaces had been exposed to the vesicle solution, and before the installation into the apparatus (in KNO_3 solution saturated with DMPC). Nevertheless, the same general long-range behavior was found. Moreover, the neutron reflectivity data (part I) clearly shows that multiple peaks are present in the reflectivity curve when vesicles are present on the bilayer (see also Majewski et al., 1998). This was *not seen* for the preparation method used for the studies carried out here (see part I).

Another possibility is that these forces arise from the underlying polymer layer. In this case, a significant swelling

of the polymer layer would have to be assumed. Swelling of the PEI layer was shown in part I, in which the layer swelled to nearly 15 nm. The long-range interaction could then be interpreted as an osmotic pressure arising when water is squeezed out from the inner aqueous compartments during the compression of the polymer cushions.

Although the short-range hemi-fusion process should be largely independent of these long-range forces, other interactions at short-to-intermediate distances may affect the intermembrane adhesion energy. The adhesion energy between the two polymer-supported DMPC bilayers was found to be at least one order of magnitude lower than values found in earlier SFA measurements on mica-supported DMPC bilayers ($E_{\text{adhesion}} \sim 0.1$ mJ/m^2) (Marra and Israelachvili, 1985). Also, the measured decay lengths of the exponential short-range repulsion between the soft-supported membranes were in the range of 7–10 Å compared to 1–3 Å for solid supported bilayers. There are several contributions to the short-range forces between free bilayers that do not arise between solid-supported bilayers. One of these is the bilayer undulation force, but it is likely that the soft polymeric cushion also induces an additional repulsive contribution. This effectively reduces the adhesion between two soft-supported bilayers, and extends the range of the steric-entropic repulsion between them, as observed. If the reduced adhesion is indeed due to membrane undulation forces, then from our findings we can estimate the bending constant of fluid DMPC bilayers. To start, there should exist a van der Waals adhesion between the phospholipids. The pressure between two such surfaces has been shown to fit well with

$$P_{\text{vdW}} = -A/(6\pi D_{\text{gap}}^3) \tag{3}$$

where D_{gap} is the bilayer separation and A is the Hamaker constant for DMPC in the fluid phase. We recall the pressure for undulatory forces originally derived by Helfrich (1978):

$$P_{\text{und}} = +(k_{\text{B}}T)^2/(2KD_{\text{gap}}^3) \tag{4}$$

where K is the elastic bending modulus of a single bilayer. Since we measure approximately zero adhesion force, we can equate these two pressures to derive an expression for the bending energy:

$$K = 3\pi(k_{\text{B}}T)^2/A \tag{5}$$

For fluid-phase DMPC, $A = 7 \times 10^{-21}$ J (Marra and Israelachvili, 1985) and at 28°C we calculate $K = 2.3 \times 10^{-20}$ J, which compares favorably with a literature-reported value $K = 3.5 \times 10^{-20}$ J (Evans and Needham, 1987).

Conclusions and future work

We have presented SFA measurements of the interaction of two polymer-cushioned lipid bilayer membranes, and for the first time have observed both hemi-fusion and complete fusion of the bilayers. The adhesion and the pressure and activation energy to achieve hemi-fusion were found to be considerably smaller for the polymer-supported system compared to solid-supported bilayers. After separation from the hemi-fused state complete healing of the membranes was observed, which points to the preserved fluidity of the system. At lower temperatures, when DMPC bilayers are in the gel state, very high pressures are needed for hemi-fusion and the healing process is very slow. This system of more natural membrane fluidity and with aqueous compartments on either side will now allow the study of membranes of increased complexity, e.g., with functional integral membrane proteins in the bilayers under more physiological conditions.

The cationic nature of the PEI layer also allows for the binding of anionic lipid headgroups onto the soft support via electrostatic (ionic) interactions or via the formation of chemical bonds between the amino groups of PEI and the headgroups of reactive membrane inserting lipids (Beyer et al., 1996; Seitz et al., 1998). Such covalent fixation provides an additional stabilization factor that would decrease membrane desorption from the polymeric substrate. This concept of "tethered supported membranes" has been discussed frequently in the literature (Häussling et al., 1991; Spinke et al., 1992; Sackmann, 1996). In addition, it is feasible that alternating polyelectrolyte multilayers can be formed by the use of polyanion "counterlayers" that would allow control of the thickness and charge of the polymeric cushion between the solid surface and the supported membrane (Decher and Hong, 1991; Lindholm-Sethson, 1996; Decher, 1997), which could be of importance for future incorporation of transmembrane proteins.

This work was funded under National Science Foundation Grant CTS-9634050, National Institutes of Health Grant GM-47334, and a National Institutes of Health-NRSA Individual Postdoctoral Fellowship Grant GM17876 (to J.Y.W.). M.S. acknowledges partial funding by the Deutsche Forschungsgemeinschaft (Fellowship Se 855/1-1).

REFERENCES

Bangham, A. D., M. W. Hill, and N. G. Miller. 1974. Preparation and use of liposomes as models of biological membranes. *Methods Membr. Biol.* 1:1–68.

Bayerl, T., and M. Bloom. 1990. Physical properties of single phospholipid bilayers adsorbed to micro glass beads. *Biophys. J.* 58:357–362.

Beyer, D., G. Elender, W. Knoll, M. Kühner, S. Maus, H. Ringsdorf, and E. Sackmann. 1996. Influence of anchor lipids on the homogeneity and mobility of lipid bilayers on thin polymer films. *Angew. Chem. Int. Ed. Engl.* 35:1682–1685.

Breisblatt, W., and S. Ohki. 1975. Fusion of phospholipid spherical membranes. I. Effect of temperature and lysolecithin. *J. Membr. Biol.* 23: 385–401.

Brian, A. A., and H. M. McConnell. 1984. Allogenic stimulation of cytotoxic T cells by supported planar membranes. *Proc. Natl. Acad. Sci. USA.* 81:6159–6163.

Chen, Y.-L., and J. N. Israelachvili. 1992. Effects of ambient conditions on adsorbed surfactant and polymer monolayers. *J. Phys. Chem.* 96: 7752–7760.

Chernomordik, L. V., G. B. Melikyan, and Y. A. Chizmadzhev. 1987. Biomembrane fusion: a new concept derived from model studies using two interacting planar lipid bilayers. *Biochim. Biophys. Acta.* 906: 309–352.

Cornell, B. A., V. L. B. Braach-Maksvytis, L. B. King, P. D. J. Osman, B. Raguse, L. Wieczorek, and R. J. Pace. 1997. A biosensor that uses ion-channel switches. *Nature*. 387:580–583.

Decher, G. 1997. Fuzzy nanoassemblies: toward layered polymeric multicomposites. *Science*. 277:1232–1237.

Decher, G., and J. D. Hong. 1991. Buildup of ultrathin multilayer films by a self-assembly process. II. Consecutive adsorption of anionic and cationic bipolar amphiphiles and polyelectrolytes on charged surfaces. *Ber. Bunsenges. Phys. Chem.* 95:1430–1434.

Decher, G., and J. Schmitt. 1992. Fine-tuning of the film thickness of ultrathin multilayer films composed of consecutively alternating layers of anionic and cationic polyelectrolytes. *Progr. Colloid Polym. Sci.* 89:160–164.

Evans, E., and D. Needham. 1987. Physical properties of surfactant bilayer membranes: thermal transitions, elasticity, rigidity, cohesion, and colloidal interactions. *J. Phys. Chem.* 91:4219–4228.

Häussling, L., W. Knoll, H. Ringsdorf, F. J. Schmitt, and J. L. Yang. 1991. Surface functionalization and surface recognition: plasmon optical detection of molecular recognition at self assembled monolayers. *Makromol. Chem., Makromol. Symp.* 46:145–155.

Helfrich, W. 1978. Steric interaction of fluid membranes in multilayer systems. *Z. Naturforsch.* 33:305–315*a* (Abstr.).

Helm, C. A., J. N. Israelachvili, and P. M. McGuiggan. 1989. Molecular mechanisms and forces involved in the adhesion and fusion of amphiphilic bilayers. *Science*. 246:919–922.

Helm, C. A., J. N. Israelachvili, and P. M. McGuiggan. 1992. Role of hydrophobic forces in bilayer adhesion and fusion. *Biochemistry*. 31: 1794–1805.

Helm, C. A., W. Knoll, and J. N. Israelachvili. 1991. Measurement of ligand-receptor interactions. *Proc. Natl. Acad. Sci. USA*. 88:8169–8173.

Heysel, S., H. Vogel, M. Sanger, and H. Sigrist. 1995. Covalent attachment of functionalised lipid bilayers to planar waveguides for measuring protein binding to biomimetic membranes. *Protein Sci.* 4:2532–2544.

Horn, R. G. 1984. Direct measurement of the force between two lipid bilayers and observation of their fusion. *Biochim. Biophys. Acta.* 778: 224–228.

Hvidt, S., and K. Heller. 1990. Viscoelastic properties of biological networks and gels. *In* Physical Networks. Polymers and Gels. W. Burchard and S. Ross-Murphy, editors. Elsevier, London. 195–208.

Israelachvili, J. 1973. Thin film studies using multiple-beam interferometry. *J. Colloid Interface Sci.* 44:259–272.

Israelachvili, J. 1987. Solvation forces and liquid structure, as probed by direct force measurements. *Acc. Chem. Res.* 20:415–421.

Israelachvili, J. 1991. Intermolecular and Surface Forces. Academic Press Ltd., London.

Israelachvili, J. N. 1989. Techniques for direct measurements of forces between surfaces in liquids at the atomic scale. *Chemtracts-Analyt. Phys. Chem.* 1:1–12.

Israelachvili, J. N., and G. E. Adams. 1976. Direct measurements of long range forces between two mica surfaces in aqueous KNO_3 solutions. *Nature*. 262:774–776.

Israelachvili, J. N., and G. E. Adams. 1978. Measurement of forces between two mica surfaces in aqueous electrolyte solutions in the range 0–100 nm. *J. Chem. Soc., Faraday Trans I*. 975–1001.

Israelachvili, J. N., and P. M. McGuiggan. 1990. Adhesion and short-range forces between surfaces. I. New apparatus for surface force measurements. *J. Mater. Res.* 5:2223–2231.

Jacobson, K., E. D. Sheets, and R. Simson. 1995. Revisiting the fluid mosaic model of membranes. *Science* 268:1441–1442.

Janiak, M. J., D. M. Small, and G. G. Shipley. 1976. Nature of the thermal pretransition of synthetic phospholipids: dimyristoyl and dipalmitoyllecithin. *Biochemistry*. 15:4575–4580.

Janmey, P. 1995. Cell membranes and the cytoskeleton. *In* Handbook of Biological Physics. R. Lipowsky and E. Sackmann, editors. Elsevier, Amsterdam. 805–849.

Kalb, E., S. Frey, and L. K. Tamm. 1992. Formation of supported planar bilayers by fusion of vesicles to supported phospholipid monolayers. *Biochim. Biophys. Acta.* 1103:307–316.

Kalb, E., and L. K. Tamm. 1992. Incorporation of cytochrome b5 into supported phospholipid bilayers by vesicle fusion to supported monolayers. *Thin Solid Films*. 210/211:763–765.

Kühner, M., R. Tampe, and E. Sackmann. 1994. Lipid mono- and bilayer-supported on polymer films: composite polymer-lipid films on solid substrates. *Biophys. J.* 67:217–226.

Lang, H., C. Duschl, M. Grätzel, and H. Vogel. 1992. Self-assembly of thiolipid molecular layers on gold surfaces: optical and electrochemical characterization. *Thin Solid Films*. 210/211:818–821.

Leckband, D. E., C. A. Helm, and J. Israelachvili. 1993. Role of calcium in the adhesion and fusion of bilayers. *Biochemistry*. 32:1127–1140.

Leckband, D. E., J. N. Israelachvili, F. J. Schmitt, and W. Knoll. 1992. Long-range attraction and molecular rearrangements in receptor-ligand interactions. *Science*. 255:1419–1421.

Leckband, D. E., F. J. Schmitt, J. N. Israelachvili, and W. Knoll. 1994. Direct force measurements of specific and nonspecific protein interactions. *Biochemistry*. 33:4611–4624.

Lindholm-Sethson, B. 1996. Electrochemistry at ultrathin organic films at planar gold electrodes. *Langmuir*. 12:3305–3314.

Lowack, K., and C. Helm. 1995. Polyelectrolyte monolayers at the mica/air interface: mechanically induced rearrangements and monolayer annealing. *Macromolecules*. 28:2912–2921.

Majewski, J., J. Y. Wong, C. K. Park, M. Seitz, J. N. Israelachvili, and G. S. Smith. 1998. Structural studies of polymer-cushioned lipid bilayers. *Biophys. J.* 76:2363–2367.

Marra, J., and J. Israelachvili. 1985. Direct measurements of forces between phosphatidylcholine and phosphatidylethanolamine bilayers in aqueous electrolyte solution. *Biochemistry*. 24:4608–4618.

McConnell, H. M., T. H. Watts, R. M. Weis, and A. A. Brian. 1986. Supported planar membranes in studies of cell-cell recognition in the immune system. *Biochim. Biophys. Acta.* 864:95–106.

Ohki, S. 1993. Fusion of spherical membranes. *In* Membrane Fusion Techniques, Part A. N. Düzgünes, editor. Academic Press, San Diego. 79–89.

Sackmann, E. 1996. Supported membranes: scientific and practical applications. *Science*. 271:43–48.

Seitz, M., C. K. Park, J. Y. Wong, and J. N. Israelachvili. 1999. Study of the fusion process between solid- and soft-supported phospholipid bilayers with the surface forces apparatus. *In* ACS Symposium Series: Supramolecular Structure in Confined Geometries. G. Warr and S. Manne, editors. Washington, D.C. In press.

Seitz, M., J. Y. Wong, C. K. Park, N. A. Alcantar, and J. N. Israelachvili. 1998. Formation of tethered supported bilayers via membrane-inserting reactive lipids. *Thin Solid Films.* 327–329:767–771.

Skehel, J. J., and D. C. Wiley. 1998. Coiled coils in both intracellular vesicle and viral membrane fusion. *Cell*. 95:871–874.

Sowers, A. E. 1987. Cell Fusion. Plenum Press, New York.

Spinke, J., J. Yang, H. Wolf, M. Liley, H. Ringsdorf, and W. Knoll. 1992. Polymer-supported bilayer on a solid substrate. *Biophys. J.* 63: 1667–1671.

Stelzle, M., G. Weissmüller, and E. Sackmann. 1993. On the application of supported bilayers as receptive layers for biosensors with electrical detection. *J. Phys. Chem.* 97:2974–2981.

Tamm, L. K., and H. M. McConnell. 1985. Supported phospholipid bilayers. *Biophys. J.* 47:105–113.

Wong, J. Y., T. L. Kuhl, J. N. Israelachvili, N. Mullah, and S. Zalipsky. 1997. Direct measurement of a tethered ligand-receptor interaction potential. *Science*. 275:820–822.

Wong, J. Y., J. Majewski, M. Seitz, C. K. Park, J. N. Israelachvili, and G. S. Smith. 1999. Polymer-cushioned bilayers. I. A structural study of various preparation methods using neutron reflectometry. *Biophys. J.* 77:1445-1457.